

Prospects for Probing Axionlike Particles at a Future Hadron Collider through Top Quark Production

Yasaman Hosseini  and Mojtaba Mohammadi Najafabadi * School of Particles and Accelerators, Institute for Research in Fundamental Sciences (IPM),
Tehran P.O. Box 19395-5531, Iran; yasaman.hosseini@cern.ch

* Correspondence: mojtaba@cern.ch

Abstract: Axionlike particles (ALPs) emerge from spontaneously broken global symmetries in high energy extensions of the Standard Model (SM). This causes ALPs to be among the objectives of future experiments that intend to search for new physics beyond the SM. We discuss the reach of future pp collider FCC-hh in probing the ALP model parameters through top quark pair production associated with ALP ($t\bar{t} + \text{ALP}$) in a model-independent approach. The search is performed in the semi-leptonic decay mode of $t\bar{t}$ and the analysis is performed using a parametric simulation of the detector response for a projected integrated luminosity of 30 ab^{-1} . It is shown that $t\bar{t} + \text{ALP}$ production at the FCC-hh is a promising channel with significant sensitivity to probe the ALP coupling with gluons. The ALP coupling with gluons obtained from HL-LHC and other experiments is presented for comparison.

Keywords: top quark; models beyond the standard model



Citation: Hosseini, Y.; Mohammadi Najafabadi, M. Prospects for Probing Axionlike Particles at a Future Hadron Collider through Top Quark Production. *Universe* **2022**, *8*, 301. <https://doi.org/10.3390/universe8060301>

Academic Editor: Jinmin Yang

Received: 29 March 2022

Accepted: 23 May 2022

Published: 26 May 2022

Publisher's Note: MDPI stays neutral with regard to jurisdictional claims in published maps and institutional affiliations.



Copyright: © 2022 by the authors. Licensee MDPI, Basel, Switzerland. This article is an open access article distributed under the terms and conditions of the Creative Commons Attribution (CC BY) license (<https://creativecommons.org/licenses/by/4.0/>).

1. Introduction

Axionlike particles (ALPs) are pseudo-Goldstone bosons that can appear from the spontaneous breaking of some global symmetries at energy scales well above the electroweak scale. In recent years, there has been much interest in ALPs because of their various notable aspects. ALPs possess many applications based on their masses and couplings in the parameter space. ALPs can solve the strong CP problem [1] and they are appropriate candidates for non-thermal Dark Matter (DM) [2]. ALPs can play a vital role in baryogenesis, giving an explanation for the observed imbalance in matter and anti-matter [3], and are able to explain the neutrino mass problem through an ALP–neutrino interaction that causes neutrinos to earn mass [4]. Furthermore, ALPs can address the muon anomalous magnetic dipole moment [5] and the excess observed in the rare K meson studies reported by the KOTO experiment [6].

ALPs are mostly probed in a model-independent effective field theory (EFT) framework. The strength of ALPs' couplings to SM fields is proportional to the inverse of $U(1)$ spontaneous symmetry breaking scale f_a , which is much higher than the electroweak symmetry breaking scale of the SM. Thus far, a remarkable region of the ALP parameter space in terms of its mass and couplings has been probed or will be studied by cosmological observations, low-energy experiments, and collider searches [7–14].

Very light ALPs with masses below the electron pair mass ($m_a < 2m_e$) are only allowed to decay into a pair of photons. Based on the ALPs' masses and couplings, heavier ones are allowed to decay into hadrons and charged leptons. The decay rates of light ALPs are usually very small, such that they can travel a long distance before they decay. Long-lived ALPs appear as invisible particles at colliders; therefore, they appear as missing energy in the detectors since they decay outside the detector environment. There are several proposals for searches at collider experiments to probe long-lived ALPs via mono-jet, mono- V ($V = \gamma, W, Z$), and jet + γ [15–22]. Searches for ALPs via exotic Higgs decays $H \rightarrow Z + a$ and $H \rightarrow a + a$ with ALP decays to diphoton and dilepton at the LHC have

provided remarkable sensitivities in a vast region of parameter space [10,11,23–25]. There are searches for ALPs through the production of dijet in association with an ALP and jet+ALP at the LHC and FCC-hh, which can be found, for instance, in Refs. [15,21]. It has been shown that the dijet+ALP channel using multivariate analysis provides strong sensitivity to the ALP coupling with gluons. Although the bounds on the ALP coupling with gluons from dijet+ALP and jet+ALP [21] are very strong, it is worth performing complementary searches through $t\bar{t} + ALP$. Furthermore, the structure of the fermionic ALP couplings is specific as it consists of the Yukawa matrices; as a result, the ALP is expected to couple more strongly to third-generation quarks. This makes $t\bar{t} + ALP$ an important channel by which to explore the ALP model.

In this paper, we propose a search for strong and fermionic couplings of ALPs through the associated production of an ALP with a pair of $t\bar{t}$ in proton–proton collisions at the future circular collider (FCC-hh) [26] at a center-of-mass energy of 100 TeV. In particular, the focus is on a region of the parameter space in which an ALP does not decay inside the detector and manifest as missing energy.

This paper is organized as follows. In Section 2, an introduction to the ALP model is presented. Section 3 is dedicated to presenting the details of the search for the ALP model using $t\bar{t} + ALP$. In Section 4, a summary of the results and discussion is given.

2. Effective Lagrangian for Axionlike Particles

The theoretical framework adopted throughout this work is a linear effective field theory where electroweak physics beyond the SM is expressed by a linear EFT expansion versus gauge-invariant operators ordered by their mass dimension. The model includes SM plus an ALP, where the scale of the new physics is the ALP decay constant f_a . The most general effective Lagrangian describing ALP interactions with SM fields up to dimension $D = 5$ operators has the following form [15]:

$$\begin{aligned} \mathcal{L}_{eff}^{D \leq 5} = & \mathcal{L}_{SM} + \frac{1}{2}(\partial^\mu a)(\partial_\mu a) - \frac{1}{2}m_a^2 a^2 + c_{a\Phi} \mathbf{O}_{a\Phi}^\psi \\ & - c_{gg} \frac{a}{f_a} G_{\mu\nu}^A \tilde{G}^{\mu\nu,A} - c_{WW} \frac{a}{f_a} W_{\mu\nu}^A \tilde{W}^{\mu\nu,A} - c_{BB} \frac{a}{f_a} B_{\mu\nu} \tilde{B}^{\mu\nu}, \end{aligned} \tag{1}$$

where

$$\mathbf{O}_{a\Phi}^\psi \equiv i(\bar{Q}_L \mathbf{Y}_U \tilde{\Phi} u_R - \bar{Q}_L \mathbf{Y}_D \Phi d_R - \bar{L}_L \mathbf{Y}_E \Phi e_R) \frac{a}{f_a} + \text{h.c.} \tag{2}$$

where e_R, d_R, u_R are $SU(2)_L$ singlets and L_L and Q_L are the $SU(2)_L$ doublets. The ALP EFT Lagrangian of Equation (1) is implemented in FeynRules [27] according to the notation of Ref. [15]. The obtained Universal FeynRules Output (UFO) model [28] (http://feynrules.irmp.ucl.ac.be/attachment/wiki/ALPsEFT/ALP_linear_UFO.tar.gz (accessed on 31 December 2021)) is embedded in MadGraph5_aMC@NLO [29] to compute the cross-sections and to generate the ALP signal events.

ALP Decays

According to the ALP interactions presented by the effective Lagrangian Equation (1), an ALP is allowed to decay into pairs of SM particles. For the MeV-scale ALPs, the decays into photons, charged leptons, and light hadrons are dominant. The diphoton decay mode is the most important one for light ALPs with mass $m_a < 2m_e = 1.022$ MeV. As m_a increases to $2m_e$ and above, the leptonic decay mode $a \rightarrow l^+ l^-$ becomes accessible. The ALP hadronic decay modes appear when $m_a > m_\pi$ and arise from the ALP decays $a \rightarrow gg$ and $a \rightarrow q\bar{q}$. The triple pion decay modes $a \rightarrow \pi^+ \pi^- \pi^0$ and $a \rightarrow \pi^0 \pi^0 \pi^0$ are the main hadronic modes for $m_a < 1$ GeV. Other ALP hadronic decay modes such as $a \rightarrow \pi^0 \gamma \gamma$ and $a \rightarrow \pi^+ \pi^- \gamma$ are suppressed with respect to $\pi^+ \pi^- \pi^0$ and $3\pi^0$ due to the presence of powers of the fine structure constant [17].

One should note that a fraction of ALPs decay inside the detector environment and consequently they do not appear as missing energy. The decay length of ALP \mathcal{L}_a is proportional to $\sqrt{\gamma^2 - 1}/\Gamma_a$, where Γ_a and γ are the total width and ALP Lorentz factor, respectively. The ALP decay probability in the detector volume is proportional to $e^{-\mathcal{L}_{\text{det}}/\mathcal{L}_a}$. \mathcal{L}_{det} is the transverse distance of the detector component from the collision point. In this study, the probability that the ALP does not decay inside the detector and escapes detection is considered event-by-event. The total width of the ALP is obtained from Ref. [30], where the chiral perturbation theory and vector meson dominance model have been used in width calculations. For instance, the decay probability for an ALP with $m_a = 10$ MeV and $|\vec{p}_a| = 242$ GeV is 0.0053, while the decay probability for an ALP with $m_a = 70$ MeV and $|\vec{p}_a| = 387$ GeV is 0.999.

3. ALP Production Associated with a Pair of Top Quarks

Top quark pair production in association with an ALP in proton–proton collisions at a center-of-mass energy of 100 TeV is used to probe the parameter space of the ALP model. As indicated previously, the focus is on the ALPs that do not decay within the detector volume and are not detected by the detectors appearing as missing momentum. Figure 1 depicts the representative Feynman diagrams for $t\bar{t} + \text{ALP}$ in proton–proton collisions.

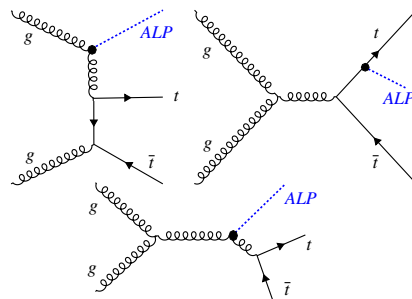


Figure 1. Representative leading order Feynman diagrams for production of a pair of top quarks with an ALP in pp collisions.

At the production level, this process is sensitive to c_{gg} and $c_{a\Phi}$. Assuming one non-vanishing ALP coupling at a time, the cross-sections $\sigma(pp \rightarrow t\bar{t} + \text{ALP})(c_{XX})$ at leading order (LO) read:

$$\begin{aligned} \sigma(c_{gg}) &= 459.6 \left(\frac{c_{gg}}{f_a}\right)^2 \text{ pb}, \\ \sigma(c_{a\Phi}) &= 2.45 \left(\frac{c_{a\Phi}}{f_a}\right)^2 \text{ pb}, \end{aligned} \tag{3}$$

where f_a is in units of TeV and the cross-sections are calculated using MadGraph5_aMC@NLO with the NNPDF23 [31] as the parton distribution functions (PDFs) of a proton. The cross-sections are obtained for the value of ALP mass $m_a = 1$ MeV and change up to 10% when m_a increases to 100 MeV. This is expected as, in this mass range, m_a is negligible in comparison to the typical energy scale of the process. The total cross-section of the SM $t\bar{t}$ production at leading order calculated by MadGraph5_aMC@NLO is 24,673.5 pb. From Equation (3), it is clear that there is more sensitivity to c_{gg} than $c_{a\Phi}$, which is due to the fact that c_{gg} appears in both initial and final states and the large gluon PDF. Since the $t\bar{t} + \text{ALP}$ rate has no significant sensitivity for $c_{a\Phi}$ coupling with respect to c_{gg} , a weaker bound on $c_{a\Phi}$ is expected.

As the ALP escapes detection, the $t\bar{t} + \text{ALP}$ can be probed through the $t\bar{t} + E_T^{\text{miss}}$ signature. A similar signature has been studied by the CMS and ATLAS collaborations in Refs. [32,33] to explore simplified models for dark matter where a mediator exists that couples to both the SM particles and dark matter. These studies investigate the production of a fermionic dark matter through a color-neutral scalar or pseudo-scalar particle (ϕ)

exchange, where the couplings between the new (pseudo)scalar and SM particles are Yukawa-like. Therefore, the mediator is expected to be produced mainly in association with heavy quarks or through loop-induced gluon–gluon fusion. The distinctive signature for dark matter in $t\bar{t} + \phi$ production followed by $\phi \rightarrow \chi\chi$, where χ is the dark matter field, is the emergence of a high missing transverse momentum recoiling against the $t\bar{t}$ system.

In this analysis, as in the past LHC search [20,32], the concentration is on the semi-leptonic $t\bar{t}$ decay channel and follows a similar selection. The final state consists of one charged lepton, four jets, and large missing transverse momentum. The main background sources to the signal arise from $t\bar{t}$, $W + jets$, $Z + jets$, single top production, and diboson. All background contributions are estimated from simulation. Both signal and background processes are generated using MadGraph5_aMC@NLO at leading order and passed through Pythia [34] to perform showering and hadronization. Delphes 3.5.0 [35], and the FCC-hh detector card (<https://github.com/delphes/delphes/blob/master/cards/FCC/FCChh.tcl> (accessed on 31 December 2021)) is used for detector simulation. The jet finding is performed using FastJet [36] using an anti- k_t algorithm with a distance parameter of 0.4 [37], considering the particle-flow reconstruction approach as described in Ref. [35]. Several signal samples are generated with ALP masses from 1 MeV to 150 MeV and f_a is taken to be 1 TeV. Based on the final state, events are selected by applying the following requirements:

- Only one isolated charged lepton (e, μ) with $p_T \geq 30$ GeV and $|\eta| \leq 2.5$. Events containing additional charged leptons with $p_T \geq 10$ GeV that fulfill loose isolation criteria are discarded. Isolated leptons are chosen with the help of the isolation variable I_{Rel} according to the definition given in Ref. [35]. Similar to Ref. [32], I_{Rel} is required to be less than 0.15 for muons and 0.035 for electrons. For loose electrons (muons), I_{Rel} is required to be less than 0.126 (0.25).
- At least three jets with $p_T \geq 30$ GeV and $|\eta| \leq 2.5$ from which one must be tagged as a b-jet. B-jet identification is based on a parametric approach that relies on Monte Carlo generator information. The probability for b-jet identification is according to the parameterization of the b-tagging efficiency available in the FCC-hh detector card. For a jet with $10 < p_T < 500$ GeV and $|\eta| < 2.5$, the b-tagging efficiency is taken to be 82% and misidentification rates are 15% and 1% for c-quark jets and light flavor jets, respectively.
- The magnitude of missing transverse momentum to be greater than 160 GeV.

For further reduction of $t\bar{t}$ and $W + jets$ backgrounds, the transverse mass $M_T = \sqrt{2p_{T,l}E_T^{\text{miss}}(1 - \cos \Delta\phi(\vec{p}_{T,l}, \vec{E}_T^{\text{miss}}))}$ has to be greater than 160 GeV. Moreover, the magnitude of the vector sum of all jets with $p_T > 20$ GeV and $|\eta| < 5.0$, H_T , is required to be larger than 120 GeV. To suppress the contribution of SM $t\bar{t}$ background, a lower cut value of 200 GeV is applied on the M_{T2}^W variable. The M_{T2}^W variable has been introduced in Ref. [38] in searches for supersymmetric partners of the top quark. To ensure the validity of the considered effective Lagrangian, it is required that its suppression scale f_a must be larger than the typical energy scale of the process. Therefore, in each event, the energy scale of the process $\sqrt{\hat{s}}$ has to be much less than f_a . In this work, the ALP appears as missing momentum and $\sqrt{\hat{s}}$ is not totally measurable. As a result, to provide the validity of the effective theory, f_a is compared to the magnitude of missing transverse momentum. The magnitude of missing transverse momentum is required to be less than f_a in each event. The signal efficiency after the cuts is found to be 12.7% for the case of $m_a = 1$ MeV. The total number of background events after the cuts corresponding to an integrated luminosity of 30 ab^{-1} is 2.12×10^7 . The signal and background efficiencies after lepton and jet selection and the cuts on M_T , M_{T2}^W , and H_T are presented in Table 1.

Table 1. Efficiency of cuts for two signal cases with $(c_{gg}/f_a = 0.1 \text{ TeV}^{-1}, m_a = 1 \text{ MeV})$; $(c_{a\Phi}/f_a = 0.1 \text{ TeV}^{-1}, m_a = 1 \text{ MeV})$, and for background processes after lepton and jet selection and applying cuts on $M_T, \text{MET}, H_T, M_{T2}^W$.

Cut	$c_{gg}/f_a = 0.1 \text{ TeV}^{-1}$	$c_{a\Phi}/f_a = 0.1 \text{ TeV}^{-1}$	$t\bar{t}$	Single Top	W+jets	Z+jets	Diboson
Lepton and jet selection, $M_T, \text{MET}, H_T, M_{T2}^W$	12.7%	3.7%	0.0077%	0.0044%	$5.65 \times 10^{-6}\%$	$5.78 \times 10^{-6}\%$	0.0046%

In order to constrain c_{XX}/f_a coupling, the first step is to set an upper limit on the signal cross-section. The expected upper 95% CL limit on the signal cross-section in the background-only hypothesis is obtained using the standard Bayesian approach [39]. Comparing the upper bound on the signal cross-section with the theoretical cross-section, the 95% CL upper limits on $|c_{XX}/f_a|$ are derived. The expected 95% CL upper bound on $|c_{gg}/f_a|$ for $m_a = 1 \text{ MeV}$ is found to be:

$$\left| \frac{c_{gg}}{f_a} \right| \leq 0.00446 \text{ TeV}^{-1} @ 30 \text{ ab}^{-1}, \tag{4}$$

The prospect at HL-LHC for $m_a = 1 \text{ MeV}$ is [20]: $\left| \frac{c_{gg}}{f_a} \right| \leq 0.063 \text{ TeV}^{-1} @ 3000 \text{ fb}^{-1}$. Excluded regions in the $(|c_{gg}/f_a|, m_a)$ plane at 95% CL from $t\bar{t} + ALP$ are presented in Figure 2. The regions are corresponding to integrated luminosities of 3000 fb^{-1} for the LHC and 30 ab^{-1} for the FCC-hh at the center-of-mass energies of 14 and 100 TeV, respectively. For the case of non-vanishing $c_{a\Phi}$ coupling, using the related signal and background efficiency in Table 1, the upper bound on $|c_{a\Phi}/f_a|$ for $m_a = 1 \text{ MeV}$ is found to be 0.11 TeV^{-1} . This limit is two orders of magnitude looser than the one derived on $|c_{gg}/f_a|$, which is due to the weaker dependence of the signal cross-section on $c_{a\Phi}/f_a$ than c_{gg}/f_a . The analysis does not have sensitivity to $|c_{gg}/f_a|$ greater than approximately 10^{-3} since, in this region, the ALP will decay inside the detector, and this is in contrast to our assumption of ALP being long-lived and detected as missing energy. Moreover, for a heavier ALP, its decay length tends to zero and, consequently, it will decay inside the detector. It is notable that the limits are obtained considering only statistical uncertainty. In the case of including systematic uncertainties similar to Ref. [32], the upper limit on $|c_{gg}/f_a|$ is weakened by around 2.2%.

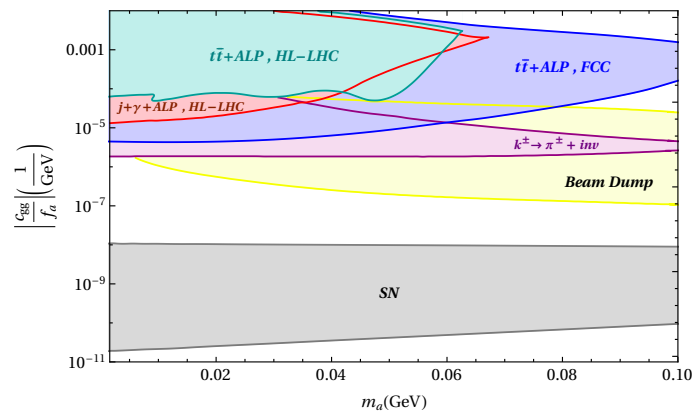


Figure 2. The expected excluded regions of the ALP model parameter space $(|c_{gg}/f_a|, m_a)$ at 95% CL obtained from $t\bar{t} + ALP$ and $j + \gamma + ALP$ channels are presented. The regions derived from $t\bar{t} + ALP$ and $j + \gamma + ALP$ processes at HL-LHC are corresponding to an integrated luminosity of 3 ab^{-1} and are adapted from Ref. [20]. The blue region shows the constraint obtained in the present analysis using $t\bar{t} + ALP$ process at FCC-hh at a center-of-mass energy of 100 TeV with an integrated luminosity of 30 ab^{-1} . The grey region denoted by SN presents the bound from supernova neutrino burst duration adapted from Ref. [7]. The region labeled by $K^\pm \rightarrow \pi^\pm + inv$ adapted from [8] (purple) and beam dump (yellow) present the constraints from Kaon decay and from the proton beam dump experiment CHARM adapted from Ref. [9].

4. Discussion

ALPs are CP odd scalar particles arising from spontaneously broken global $U(1)$ symmetries that can address some of the SM shortcomings, such as the strong CP problem, baryon asymmetry, neutrino mass, and dark matter. The potential of $t\bar{t} + ALP$ production to probe the parameter space of light ALPs at FCC-hh is studied. In general, light ALPs have a long lifetime and do not decay inside the detector, appearing as missing momentum in the final state. For the ALP mass $m_a = 1$ MeV, the obtained upper limit on ALP coupling with gluons $|c_{gg}/f_a|$ at FCC-hh is found to be 0.00446 TeV^{-1} . This bound corresponds to the ultimate integrated luminosity that the FCC-hh will eventually operate at based on the benchmark specifications. As seen in Figure 2, the limit on $|c_{gg}/f_a|$ varies slightly as the ALP mass increases. In order to compare the limits obtained in this analysis with those already derived at HL-LHC, the expected upper limits on $|c_{gg}/f_a|$ at 95% CL from $t\bar{t} + ALP$ and $j + \gamma + ALP$ are presented in Figure 2. A comparison shows that the constraints obtained from FCC-hh are stronger than the limits derived from $t\bar{t} + ALP$ and $j + \gamma + ALP$ analyses at HL-LHC by one to three orders of magnitude depending on the ALP mass. Results of Figure 2 indicate that the analysis of $t\bar{t} + ALP$ FCC-hh is able to span a large area in the ALP parameter space that is not accessible by $K^\pm \rightarrow \pi^\pm + inv$, SN, and beam dump experiments. It can be concluded that the $t\bar{t} + ALP$ production at FCC-hh provides an excellent solution in exploring the light ALP physics as a significant portion of the parameter space is accessible through this channel.

Author Contributions: All authors have equally contributed to all the parts of the manuscript. All authors have read and agreed to the published version of the manuscript.

Funding: This research received no external funding.

Data Availability Statement: Not applicable.

Acknowledgments: The authors are grateful to Yotam Soreq for the insightful comments and for providing data of Ref. [30]. The authors would also like to thank Pedro Ferreira da Silva and Efe Yazgan for inviting us to contribute to the open-access Special Issue, *Top Quark at the New Physics Frontier*.

Conflicts of Interest: The authors declare no conflict of interest.

References

1. Hooft, G. Symmetry Breaking Through Bell-Jackiw Anomalies. *Phys. Rev. Lett.* **1976**, *37*, 8–11. [[CrossRef](#)]
2. Dolan, M.J.; Kahlhoefer, F.; McCabe, C.; Schmidt-Hoberg, K. A taste of dark matter: Flavour constraints on pseudoscalar mediators. *J. High Energy Phys.* **2015**, *3*, 171; Erratum in *J. High Energy Phys.* **2015**, *7*, 103. [[CrossRef](#)]
3. Jeong, K.S.; Jung, T.H.; Shin, C.S. Adiabatic electroweak baryogenesis driven by an axionlike particle. *Phys. Rev. D* **2020**, *101*, 035009. [[CrossRef](#)]
4. Chen, C.S.; Tsai, L.H. Peccei-Quinn symmetry as the origin of Dirac Neutrino Masses. *Phys. Rev. D* **2013**, *88*, 055015. [[CrossRef](#)]
5. Chang, D.; Chang, W.F.; Chou, C.H.; Keung, W.Y. Large two loop contributions to $g-2$ from a generic pseudoscalar boson. *Phys. Rev. D* **2001**, *63*, 091301. [[CrossRef](#)]
6. Kitahara, T.; Okui, T.; Perez, G.; Soreq, Y.; Tobioka, K. New physics implications of recent search for $K_L \rightarrow \pi^0 \nu \bar{\nu}$ at KOTO. *Phys. Rev. Lett.* **2020**, *124*, 071801. [[CrossRef](#)]
7. Fukuda, H.; Harigaya, K.; Ibe, M.; Yanagida, T.T. Model of visible QCD axion. *Phys. Rev. D* **2015**, *92*, 015021. [[CrossRef](#)]
8. Izaguirre, E.; Lin, T.; Shuve, B. Searching for Axionlike Particles in Flavor-Changing Neutral Current Processes. *Phys. Rev. Lett.* **2017**, *118*, 111802. [[CrossRef](#)]
9. Döbrich, B.; Jaeckel, J.; Kahlhoefer, F.; Ringwald, A.; Schmidt-Hoberg, K. ALPtraum: ALP production in proton beam dump experiments. *J. High Energy Phys.* **2016**, *2*, 018. [[CrossRef](#)]
10. Chatrchyan, S.; Khachatryan, V.; Sirunyan, A.M.; Tumasyan, A.; Adam, W.; Aguilo, E. Search for a Non-Standard-Model Higgs Boson Decaying to a Pair of New Light Bosons in Four-Muon Final States. *Phys. Lett. B* **2013**, *726*, 564–586. [[CrossRef](#)]
11. Chatrchyan, S.; Khachatryan, V.; Sirunyan, A.M.; Tumasyan, A.; Adam, W.; Aguilo, E. Search for light bosons in decays of the 125 GeV Higgs boson in proton-proton collisions at $\sqrt{s} = 8$ TeV. *J. High Energy Phys.* **2017**, *10*, 76. [[CrossRef](#)]
12. Liu, J.; Dona, K.; Hoshino, G.; Knirck, S.; Kurinsky, N.; Malaker, M. Broadband Solenoidal Haloscope for Terahertz Axion Detection. *Phys. Rev. Lett.* **2022**, *128*, 131801. [[CrossRef](#)] [[PubMed](#)]
13. Aad, G.; Abbott, B.; Abbott, D.C.; Abed, A.; Abeling, K.; Abhayasinghe, D.K. Measurement of light-by-light scattering and search for axion-like particles with 2.2 nb^{-1} of Pb+Pb data with the ATLAS detector. *J. High Energy Phys.* **2021**, *11*, 50. [[CrossRef](#)]

14. Sirunyan, A.M.; Erbacher, R.; Carrillo Montoya, C.A.; Carvalho, W.; Górski, M.; Kotlinski, D. Evidence for light-by-light scattering and searches for axion-like particles in ultraperipheral PbPb collisions at $\sqrt{s_{NN}} = 5.02$ TeV. *Phys. Lett. B* **2019**, *797*, 134826. [[CrossRef](#)]
15. Brivio, I.; Gavela, M.B.; Merlo, L.; Mimasu, K.; No, J.M.; del Rey, R.; Sanz, V. ALPs Effective Field Theory and Collider Signatures. *Eur. Phys. J. C* **2017**, *77*, 572. [[CrossRef](#)] [[PubMed](#)]
16. Mimasu, K.; Sanz, V. ALPs at Colliders. *J. High Energy Phys.* **2015**, *6*, 173. [[CrossRef](#)]
17. Bauer, M.; Neubert, M.; Thamm, A. Collider Probes of Axion-Like Particles. *J. High Energy Phys.* **2017**, *12*, 44. [[CrossRef](#)]
18. Bonilla, J.; Brivio, I.; Machado-Rodríguez, J.; de Trocóniz, J.F. Nonresonant Searches for Axion-Like Particles in Vector Boson Scattering Processes at the LHC. *arXiv* **2022**, arXiv:2202.03450.
19. Bauer, M.; Neubert, M.; Renner, S.; Schnubel, M.; Thamm, A. Flavor probes of axion-like particles. *arXiv* **2021**, arXiv:2110.10698.
20. Ebadi, J.; Khatibi, S.; Mohammadi Najafabadi, M. New probes for axionlike particles at hadron colliders. *Phys. Rev. D* **2019**, *100*, 015016. [[CrossRef](#)]
21. Haghghat, G.; Haji Raissi, D.; Mohammadi Najafabadi, M. New collider searches for axionlike particles coupling to gluons. *Phys. Rev. D* **2020**, *102*, 115010. [[CrossRef](#)]
22. Bauer, M.; Heiles, M.; Neubert, M.; Thamm, A. Axion-Like Particles at Future Colliders. *Eur. Phys. J. C* **2019**, *79*, 74. [[CrossRef](#)]
23. Bauer, M.; Neubert, M.; Thamm, A. LHC as an Axion Factory: Probing an Axion Explanation for $(g - 2)_\mu$ with Exotic Higgs Decays. *Phys. Rev. Lett.* **2017**, *119*, 031802. [[CrossRef](#)]
24. Aad, G.; Abbott, B.; Abbott, D.C.; Abud, A.A.; Abeling, K.; Abhayasinghe, D.K. Search for new phenomena in events with an energetic jet and missing transverse momentum in pp collisions at $\sqrt{s} = 13$ TeV with the ATLAS detector. *Phys. Rev. D* **2021**, *103*, 112006. [[CrossRef](#)]
25. Aad, G.; Abbott, B.; Abbott, D.; Abed, A.; Abeling, K.; Abhayasinghe, D. Search for Higgs boson decays into a pair of pseudoscalar particles in the $bb\mu\mu$ final state with the ATLAS detector in pp collisions at $\sqrt{s} = 13$ TeV. *Phys. Rev. D* **2022**, *105*, 012006. [[CrossRef](#)]
26. FCC Collaboration. FCC-hh: The Hadron Collider: Future Circular Collider Conceptual Design Report Volume 3. *Eur. Phys. J. Spec. Top.* **2019**, *228*, 755–1107. [[CrossRef](#)]
27. Alloul, A.; Christensen, N.D.; Degrande, C.; Duhr, C.; Fuks, B. FeynRules 2.0—A complete toolbox for tree-level phenomenology. *Comput. Phys. Commun.* **2014**, *185*, 2250–2300. [[CrossRef](#)]
28. Degrande, C.; Duhr, C.; Fuks, B.; Grellscheid, D.; Mattelaer, O.; Reiter, T. UFO—The Universal FeynRules Output. *Comput. Phys. Commun.* **2012**, *183*, 1201–1214. [[CrossRef](#)]
29. Alwall, J.; Herquet, M.; Maltoni, F.; Mattelaer, O.; Stelzer, T. MadGraph 5: Going Beyond. *J. High Energy Phys.* **2011**, *6*, 128. [[CrossRef](#)]
30. Aloni, D.; Soreq, Y.; Williams, M. Coupling QCD-Scale Axionlike Particles to Gluons. *Phys. Rev. Lett.* **2019**, *123*, 031803. [[CrossRef](#)] [[PubMed](#)]
31. Ball, R.D.; Bertone, V.; Carrazza, S.; Deans, C.S.; Del Debbio, L.; Forte, S. Parton distributions with LHC data. *Nucl. Phys. B* **2013**, *867*, 244–289. [[CrossRef](#)]
32. Sirunyan, A.M.; Tumasyan, A.; Adam, W.; Asilar, E.; Bergauer, T.; Brstetter, J. Search for dark matter produced in association with heavy-flavor quark pairs in proton-proton collisions at $\sqrt{s} = 13$ TeV. *Eur. Phys. J. C* **2017**, *77*, 845. [[CrossRef](#)] [[PubMed](#)]
33. Aaboud, M.; Aad, G.; Abbott, B.; Abeloos, B.; Abidi, S.H.; AbouZeid, O.S. Search for dark matter produced in association with bottom or top quarks in $\sqrt{s} = 13$ TeV pp collisions with the ATLAS detector. *Eur. Phys. J. C* **2018**, *78*, 18. [[CrossRef](#)]
34. Sjostrand, T.; Mrenna, S.; Skands, P.Z. PYTHIA 6.4 Physics and Manual. *J. High Energy Phys.* **2006**, *5*, 26. [[CrossRef](#)]
35. de Favereau, J.; Delaere, C.; Demin, P.; Giammanco, A.; Lemaître, V.; Mertens, A.; Selvaggi, M. DELPHES 3, A modular framework for fast simulation of a generic collider experiment. *J. High Energy Phys.* **2014**, *2*, 57. [[CrossRef](#)]
36. Cacciari, M.; Salam, G.P.; Soyez, G. FastJet User Manual. *Eur. Phys. J. C* **2012**, *72*, 1896. [[CrossRef](#)]
37. Cacciari, M.; Salam, G.P.; Soyez, G. The anti- k_t jet clustering algorithm. *J. High Energy Phys.* **2008**, *4*, 63. [[CrossRef](#)]
38. Bai, Y.; Cheng, H.C.; Gallicchio, J.; Gu, J. Stop the Top Background of the Stop Search. *J. High Energy Phys.* **2012**, *7*, 110. [[CrossRef](#)]
39. Bertram, I.; Landsberg, G.L.; Linnemann, J.; Partridge, R.; Paterno, M.; Prosper, H.B. *A Recipe for the Construction of Confidence Limits*; Fermi National Accelerator Lab.: Batavia, IL, USA, 2000. [[CrossRef](#)]